



US 20080139931A1

(19) **United States**

(12) **Patent Application Publication**
Butz et al.

(10) **Pub. No.: US 2008/0139931 A1**

(43) **Pub. Date: Jun. 12, 2008**

(54) **TEMPERATURE MAPPING ON STRUCTURAL DATA**

(75) Inventors: **Torsten Butz**, Niederteufen (CH);
Jean-Philippe Thiran, St-Legier (CH);
Murat Kunt, Grandvaux (CH)

Correspondence Address:
Clifford W. Browning
Woodard, Emhardt et al. LLP
Bank One Center/Tower, 111 Monument Circle,
Suite 3700
Indianapolis, IN 46204-5137

(73) Assignee: **ImaSys SA**, Lausanne (CH)

(21) Appl. No.: **11/795,457**

(22) PCT Filed: **Jan. 13, 2006**

(86) PCT No.: **PCT/CH2006/000033**

§ 371 (c)(1),
(2), (4) Date: **Jul. 17, 2007**

(30) **Foreign Application Priority Data**

Jan. 17, 2005 (EP) 05405026.5

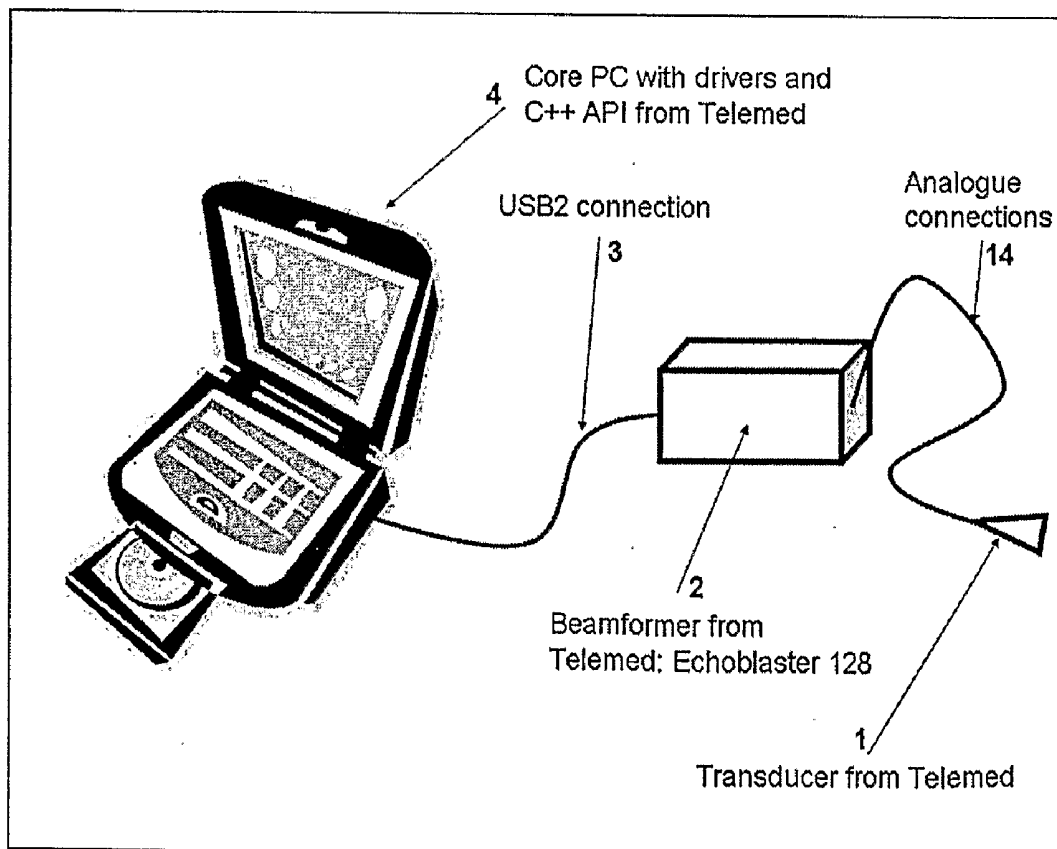
Publication Classification

(51) **Int. Cl.**
A61B 5/00 (2006.01)
A61B 8/00 (2006.01)

(52) **U.S. Cl.** **600/427; 382/131**

(57) **ABSTRACT**

Temperature imaging has been recognized to improve a variety of diagnostic and interventional procedures and to predict and prevent failures of electrical circuits and equipments. A system design and method is disclosed, wherein the thermal data is fused and mapped with the data streams coming from a US, CT, or MR scanner, giving the doctors or industrial investigators the impression of being working with a known US, CT, or MR system which has been augmented by the temperature mapping capability.



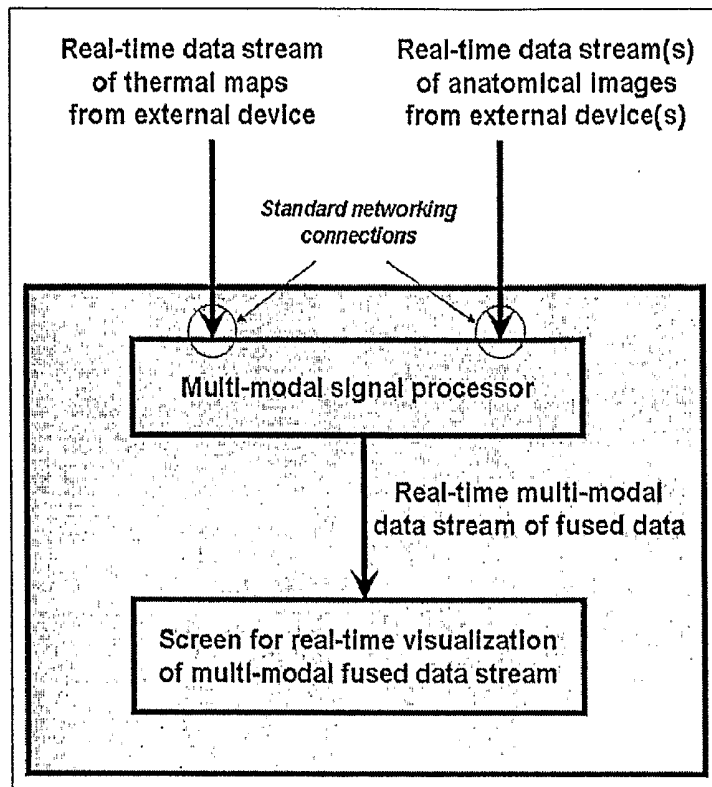


Fig. 1

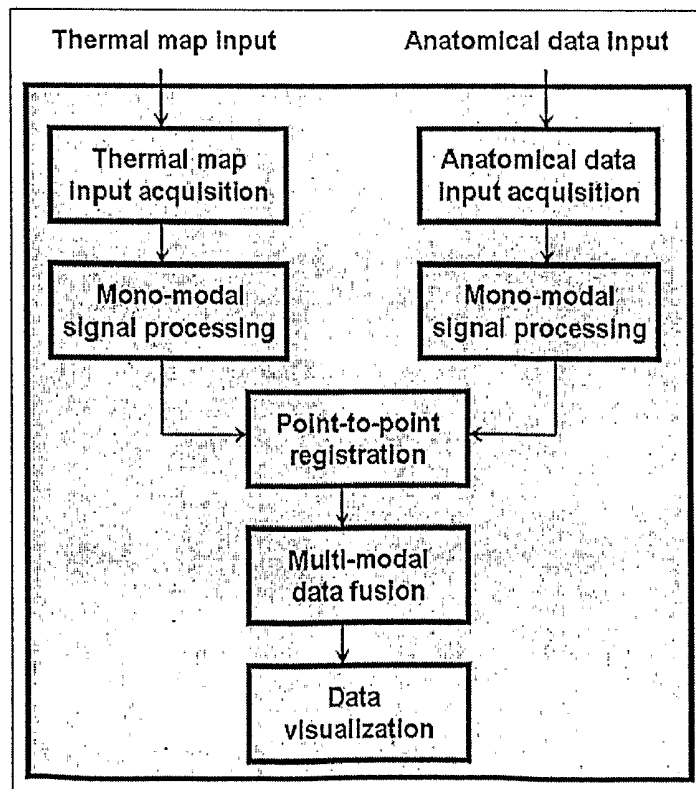


Fig. 2

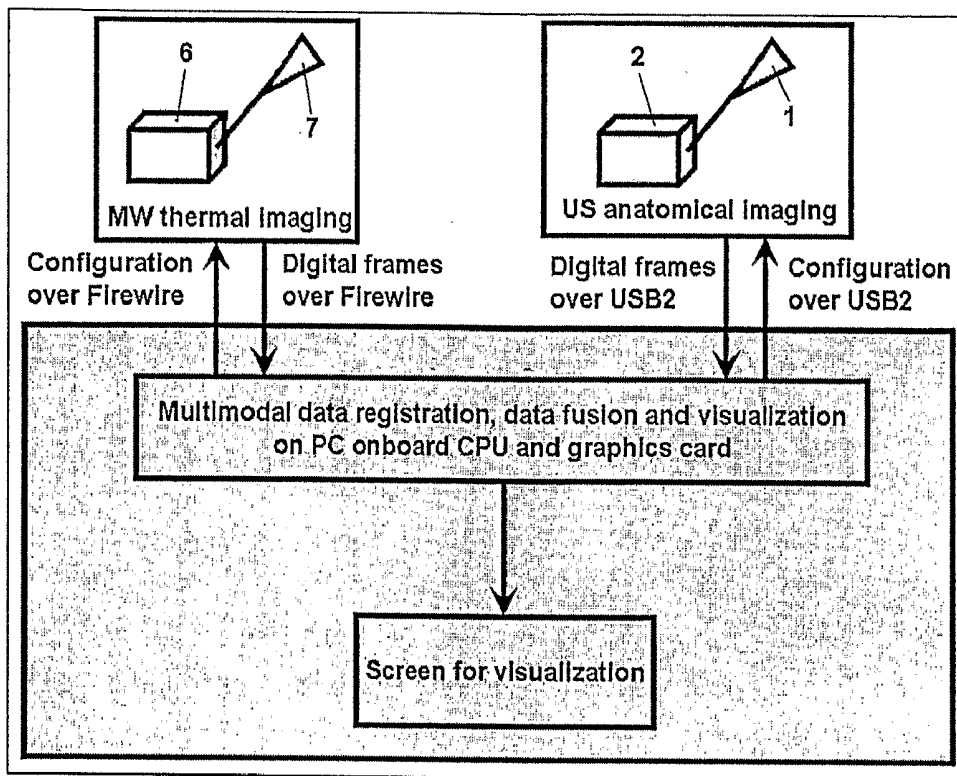


Fig. 3

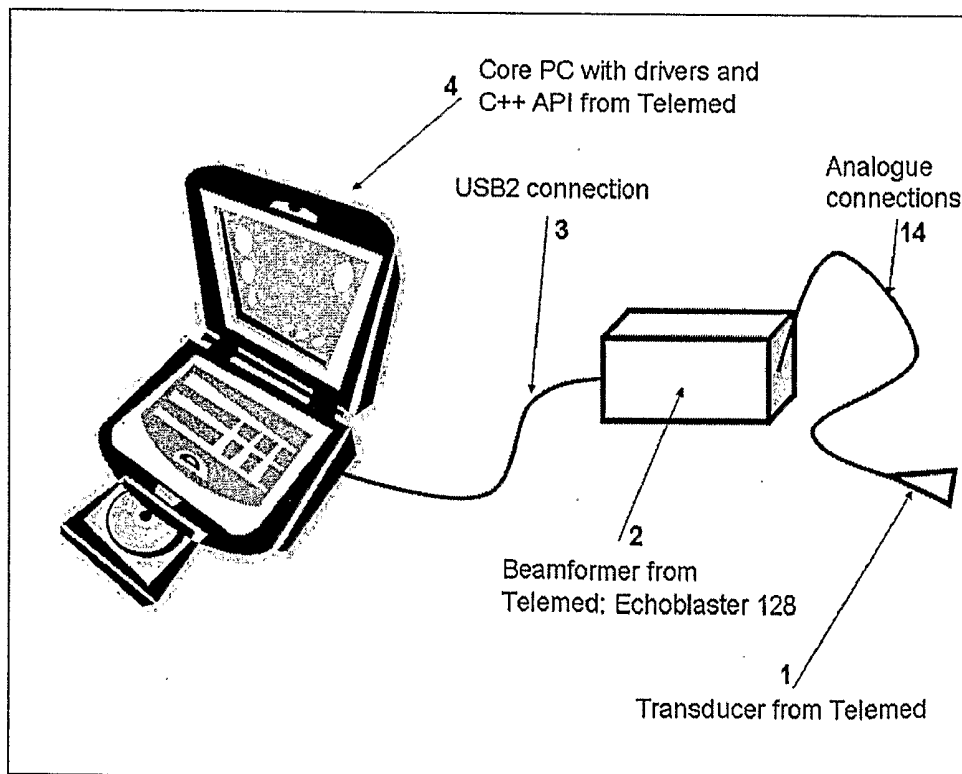


Fig. 4

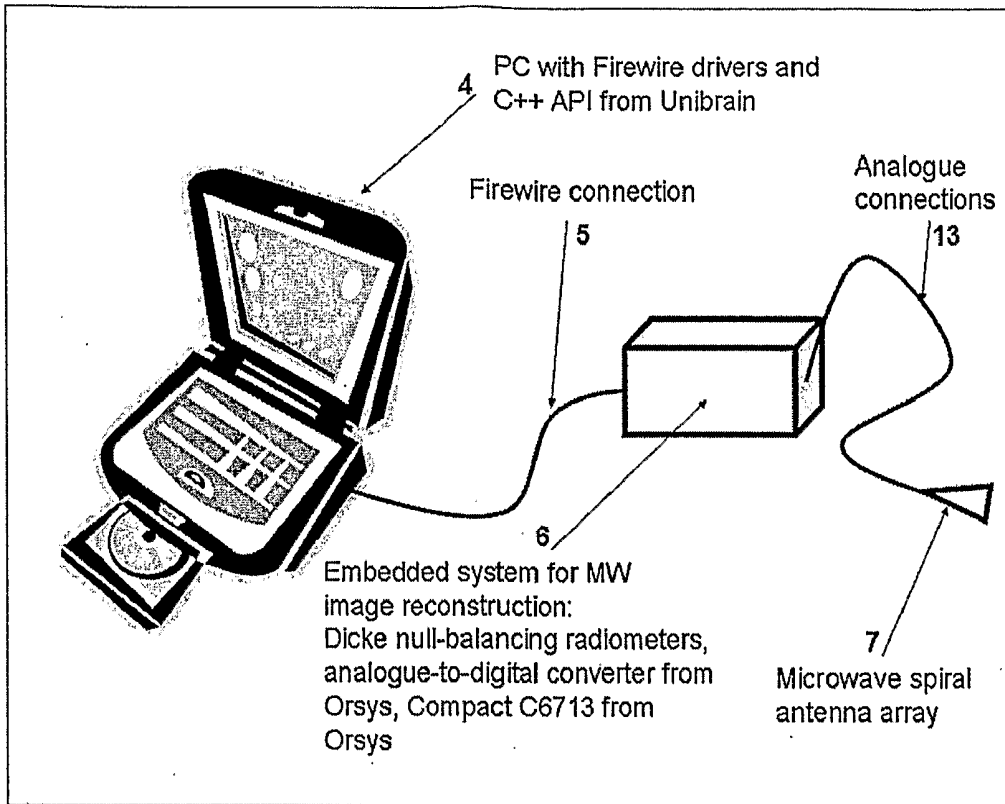


Fig. 5

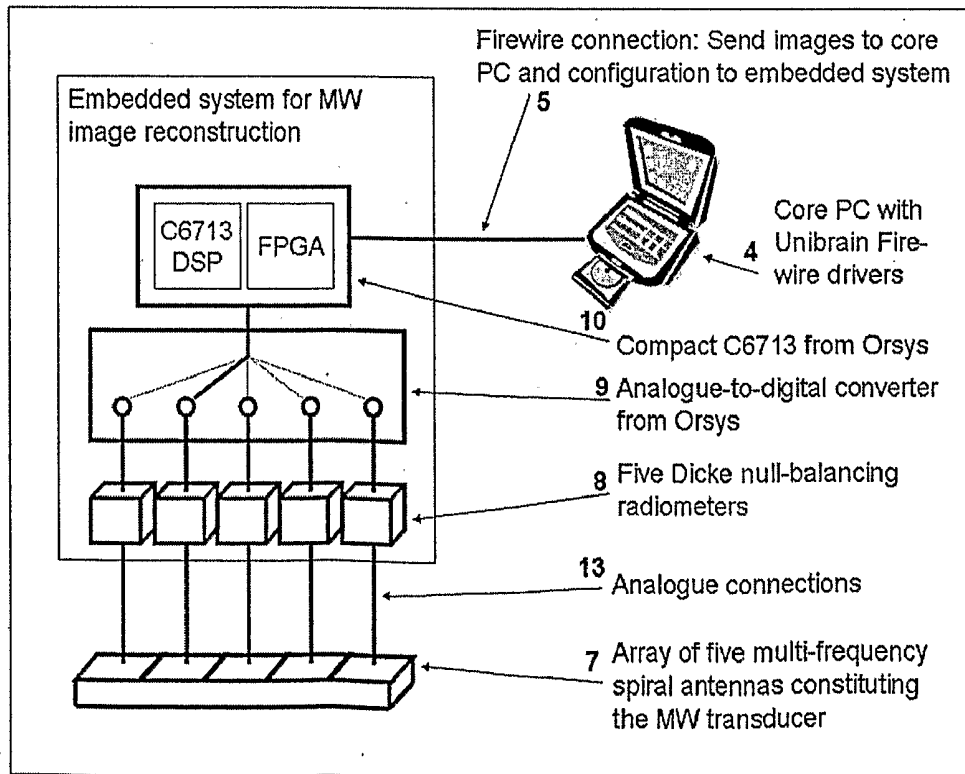


Fig. 6

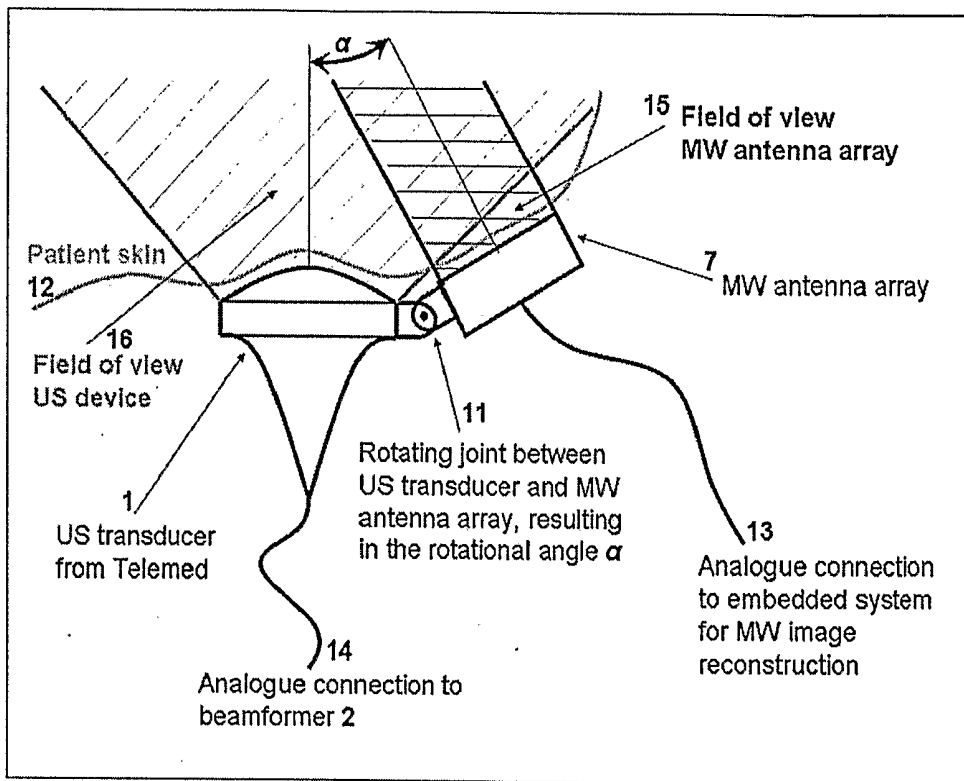


Fig. 7

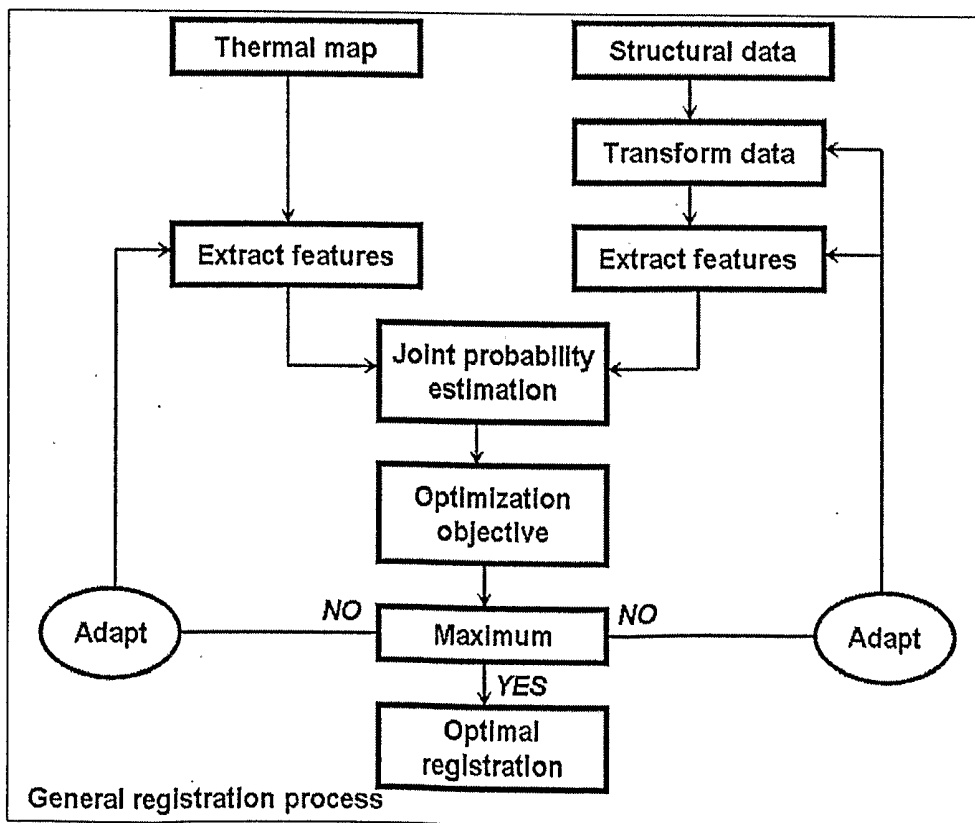


Fig. 8

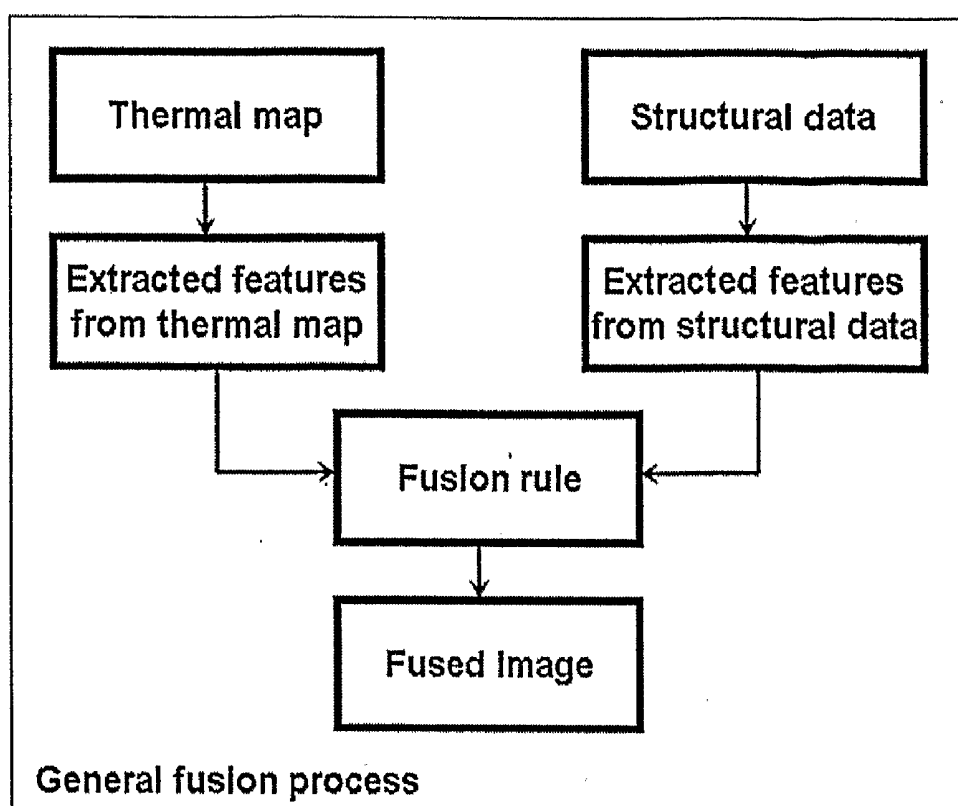


Fig. 9

TEMPERATURE MAPPING ON STRUCTURAL DATA

BACKGROUND OF THE INVENTION

[0001] Non-Destructive Evaluation (NDE) has been one of the engineering disciplines which has mostly revolutionized diagnostic techniques in industry and in medicine during the last decades. MR (Magnetic Resonance), CT (Computerized Tomography), US (Ultra-Sound), and other NDE devices are being standard tools for a wide range of diagnostic fields. Furthermore they are currently changing significantly medical surgery, as their capability of visualizing intra-body structures enables surgeons to minimize the invasiveness of their interventions. Even though NDE techniques are by themselves expensive, they are potentially even interesting from a financial point of view, as they can significantly decrease the expensive hospitalization time of patients. Similar arguments apply to industrial NDE which was able to bring quality assurance and failure prediction to an impressive performance.

[0002] Information coming from one NDE device is always restricted to a particular characteristic of the intra-body physics. For example, the information that can be drawn from MR devices or CT scanners is related but still very different. While medical MR devices image the soft tissues, CT scanners are unable to discriminate different types of soft tissues while giving information about the skeleton structure of the patient. In practice, both imaging systems are therefore used in conjunction when necessary, in order to exploit the complementary information provided by both devices. The result is multimodal information, i.e. information which can practically not be provided by one single system.

[0003] As used herein, "multimodal" means use of at least two imaging modes which differ by the physical characteristics of the scene they image during the data acquisition process.

[0004] One of nowadays main research directions consists of determining new imaging modalities which are able to measure more intra-body characteristics. One of these characteristics is the intra-body temperature of industrial specimen or patients. Temperature is a highly discriminative characteristic for e.g. cancer tissues or design errors in electrical circuits. Several approaches to temperature imaging have been proposed, but just few have been able to reach any real market value.

[0005] Devices enabling data acquisition of thermal maps comprise MR scanners (intra-body), infrared devices (surface), and passive microwave imaging systems (intra-body). Thermal maps are considered to give pertinent information. In the case of medical imaging, the temperature maps acquired by the imaging device can give information about the intra-body temperature distribution during thermal ablation of e.g. a tumour, or about the presence, respectively absence, of cancerous tissues in human bodies. In the context of industrial applications, thermal maps are particularly valuable for instance for the prediction and prevention of electrical equipment circuit failures.

[0006] But temperature by itself has just a restricted practical value if not combined with other imaging modalities such as US, CT, or MR data, in order not only to give intra-body temperature maps, but also to relate them to the underlying physical structure of the patient or specimen under study. For example, increased intra-body temperature is not sufficient to conclude on the presence of cancerous tissue due

to the inhomogeneity of biological tissue. It could also come from a local inflammation of the biological tissue. Underlying anatomical data reflecting this inhomogeneity can therefore increase significantly the diagnostic specificity of the acquired temperature maps.

[0007] Thermal maps are thus medically and industrially most useful in conjunction with anatomical or structural images in order to provide the medical doctors and investigators with information complementary to the thermal data. In the case of cancer detection, the anatomical images acquired by e.g. US or CT devices ensure that not only cancerous tissues are detected, but also they define their exact anatomical location, enabling the medical doctors to optimize their treatment plans. In the context of electrical circuits, the temperature maps get expressive when being related to the underlying circuit design.

[0008] Presently, different imaging modalities, such as thermal maps and anatomical information, could only be provided sequentially, but not simultaneously. As a result, the following disadvantages of existing approaches to thermal imaging can be listed:

[0009] First, anatomical and structural information is a fundamental prerequisite for medical doctors and investigators during medical diagnosis or industrial quality testing in order to locate sensitive anatomical structures, e.g. during thermal ablation, or to relate failure sensitive regions of an integrated circuit to the underlying circuit design which can be improved thereafter. Therefore, having access to mere temperature maps without having simultaneously the related structural information is a highly limiting factor, as temperature maps by themselves do not provide any information about the underlying structure.

[0010] Second, in the case of medical applications, the medical doctors are used to inspect anatomical data, but do not have much practical experience in interpreting thermal maps due to the novelty of thermal imaging devices. Therefore an appropriate combination of thermal maps with conventional anatomical imaging modalities would heavily facilitate the medical doctors' tasks of interpreting the acquired thermal maps.

[0011] Third, if thermal and structural information are acquired in a sequential manner, it is required to physically fix the patient or the investigated industrial piece during and between the successive imaging processes and to exactly determine the position of target with respect to the imaging devices in order to be able to fuse and visualize the multimodal data sets without mutual displacements.

[0012] Fourth, even if both data from the same body portion could be acquired simultaneously by two different imaging devices, a pure superimposition of the resulting images would not be optimal, as redundant or irrelevant information would get displayed as well.

[0013] Fifth, the only device currently being in practical use for the non-invasive determination of intra-body temperatures is MR. This is a very large and expensive device not being easily accessible by the majority of medical doctors.

SUMMARY OF THE INVENTION

[0014] The present invention solves the problems described above by providing means to optimally fuse and visualize the data coming from individual imaging devices.

[0015] An object of the invention is a virtual multimodal non-invasive imaging device comprising:

[0016] a first monomodal, non-invasive microwave imaging subsystem with first sensing means and with first processing means, providing digitized intra-body microwave (MW) thermal map data from a sensed body,

[0017] a second monomodal, non-invasive imaging subsystem with second sensing means and with second processing means, providing digitized intra-body structural map data from said sensed body, and

[0018] a multimodal signal processor performing spatial registration of thermal and structural maps, data fusion into a multimodal data set and visualisation of said multimodal data set,

wherein said multimodal signal processor (4) includes a feature extraction which detects and selects the image features most pertinent for the spatial correspondence of the input images.

[0019] As used herein, "spatial registration" refers to bringing two datasets into spatial correspondence, i.e. for every position in one dataset the corresponding position in the second dataset is known.

[0020] Thus, the processing system which receives the data streams from the respective imaging devices performs signal conditioning, image registration, and data fusion, in order to provide the information from the plurality of input data streams in a virtually fused single data stream.

[0021] Preferably, said processor extracts corresponding image features of said thermal map and of said structural map for the registration process. The resulting digital data stream guarantees a spatial correspondence of the input data streams from the different imaging devices.

[0022] Preferably, said processor extracts complementary image features of said thermal map and of said structural map for the data fusion step. Thereby, the system removes redundant information from the different data streams in order to guarantee the visualization of both a complete and very compact representation of all the information coming from the different input data streams.

[0023] Preferably, the thermal data of said multimodal data set are color coded and overlaid to the structural data. The system visualizes the resulting single data stream on a computer screen.

[0024] Preferably, configuration information is streamed back from said processing system to said imaging subsystems.

[0025] The system has several inputs for the different imaging devices, one of which provides the thermal data, the other(s) the complementary structural information. Data streams from the thermal imaging device and one, or more than one, structural imaging device are streamed over standard networking and data streaming connections, such as USB2, IEEE1394, Ethernet, S-Video, or others, towards the processing system. In the case of analogue streaming connections, such as S-Video, a state-of-the-art analogue-to-digital converter or frame-grabber digitizes the analogue data before passing the resulting digital representation to the processor.

[0026] In order to bring the data into spatial correspondence, the imaging devices can be linked mechanically and calibrated to pre-determine the transformation which brings the data into correspondence. The resulting transformation can thereafter be applied in real-time. As an alternative, a software tool performs this spatial registration task by maximizing an information theoretic measure between image fea-

tures with respect to possible image rotations and displacements. Further, the software will extract the most complementary and pertinent image features and characteristics of the different image modalities before fusing the resulting data into one multi-modal data set. As a final step, the resulting image representing the multimodal information is being visualized on a computer screen.

[0027] As used herein "real-time" capability of the final system refers to a real-time capability which does not significantly differ from the real-time capabilities of the individual imaging subsystems which are connected to the core device.

[0028] As used herein, "information theoretic measures" refer to all functionals constructed from information theoretic statistics, such as entropy, joint entropy, mutual information etc.

[0029] The system streams two data streams to the signal processor, e.g. the 2D thermal data from a MW thermal imaging device, noted $T(x,y)$, and the 2D structural data from a structural imaging device, noted $S(x',y')$, where x and y , resp. x' and y' , parameterize the discrete imaging space of the thermal MW data T , resp. the structural data S . A mapping $m_\alpha: (x',y') \rightarrow (x,y)$ provides a spatial correspondence between both, the imaging space of T and the imaging space of S , with α being the registration parameters for rigid or non-rigid registration, e.g. α parameterizes translations and rotations of the 2D structural data frames in 3D to register them with the thermal map. Analogously, the mapping might be from the temperature imaging space to the structural data imaging space: $m_{\alpha'}: (x,y) \rightarrow (x',y')$. Then, α' parameterizes translations and rotations of the 2D MW data frames. The mapping parameters α and image features which allow the determination of α have to be determined simultaneously. Mathematically, the feature extraction can be formalized as an image mapping, $k_\beta: T(x,y) \rightarrow k_\beta(T(x,y))$, resp. $l_\gamma: S(x',y') \rightarrow l_\gamma(S(x',y'))$, with β , resp. γ , being the feature extraction parameters. The aim of using image features instead of the raw image data for the registration process reflects the fact that not all information contained in multimodal data is pertinent for the registration process. Some image characteristics solely present in one of the modalities, such as imaging noise, cannot give any reliable input to the registration process, but rather decrease reliability of the algorithm. Therefore the feature extraction block within the multimodal registration process detects the image features most pertinent for the spatial correspondence of the input images and removes those not being of any use for this aim.

[0030] The optimization objective which allows simultaneous extraction of the most related image features and the determination of the optimal registration parameters α is written

$$e(F_T, F_S) = I(F_T, F_S) / H(F_S, F_T).$$

[0031] This functional is called feature efficiency. $I(...)$ stands for mutual information, $H(...)$ for joint entropy, F_T is a random variable with a probability density p_T estimated from the features of the thermal data T , and F_S is a random variable with a probability density p_S estimated from the features of the structural data S . Using histogramming, the following formulas are being employed to estimate the probability densities, p_S , p_T , and joint probability $p_{S,T}$, for the random variables, F_S , F_T , and joint random variable $F_{S,T}$, respectively. f_S

and f_T are the features extracted from the data S and T, respectively:

$$p_S(f_S) = \frac{1}{N} \sum_{x,y} \delta_{f_S(x,y),f_S},$$

$$p_T(f_T) = \frac{1}{N} \sum_{x,y} \delta_{f_T(x,y),f_T},$$

$$p_{S,T}(f_S, f_T) = \frac{1}{N} \sum_{x,y} \delta_{f_S(x,y),f_S} \delta_{f_T(x,y),f_T},$$

where N is the number of features extracted from the datasets, and $\delta_{a,b}$ is the Kronecker delta function, which is 1 if $a=b$ and 0 otherwise. Other probability estimators might be used as well, such as Parzen-window probability estimation. This probability estimation step is important to the registration process of FIG. 8. Afterwards, information theoretic measures can be evaluated and optimized using these probability densities.

[0032] Using these definitions, the exact expressions for mutual information and entropy can be given:

$$I(F_S, F_T) = \sum_{f_S} \sum_{f_T} p_{S,T}(f_S, f_T) \log \frac{p_{S,T}(f_S, f_T)}{p_S(f_S) p_T(f_T)}$$

$$H(F_S) = \sum_{f_S} p_S(f_S) \log(p_S(f_S)).$$

[0033] In FIG. 8, just the joint probability estimation is being included in the block diagram. This is because the marginal probability densities, p_S and p_T , can alternatively be calculated directly from the joint probability density, $p_{S,T}$, evaluated itself by histogramming.

[0034] As an alternative to feature efficiency, normalized entropy might be used to drive the optimization process. It is defined by:

$$NE(F_T, F_S) = ((H(F_T) + H(F_S)) / H(F_S, F_T)).$$

[0035] In the case of feature efficiency, the resulting data registration process can be formalized as

$$(\alpha^{opt}, \beta^{opt}, \gamma^{opt}) = \max_{\alpha, \beta, \gamma} e^{(F_{\alpha\beta\gamma}(T(m_{\alpha}(x,y))), F_{\gamma}(S(x',y'))))}.$$

[0036] This process is outlined in FIG. 8. The action of adapting registration parameters and image features refers to adapting the parameters α , β , and γ . For maximization, any adequate optimization algorithm can be used.

[0037] In contrast to the first data feature extraction related to image registration as described in the previous paragraph, the second feature extraction for data fusion aims to extract the features of the initial datasets which are most complementary to each other while removing redundant information from the datasets. Mathematically, the feature extraction process is written the same way as in the previous paragraph, even though its implementation might differ. Therefore, the feature extraction from the input thermal and structural maps is represented by a mapping $o_{\delta}: T(m_{\alpha}(x,y)) \rightarrow o_{\delta\gamma}(T(m_{\alpha}(x,y))),$ resp. $u_{\epsilon}: S(x',y') \rightarrow u_{\epsilon}(S(x',y'))$. δ , resp. ϵ , represent again feature extraction parameters of the initial MW thermal map, $T(x,y)$, resp. of the structural data device, $S(x',y')$. The extrac-

tion process is driven by the minimization of the same optimization function as in the previous paragraph. Mathematically this can be written

$$(\delta^{opt}, \epsilon^{opt}) = \min_{\delta, \epsilon} e^{(F_{\alpha\delta}(T(m_{\alpha}(x,y))), F_{u\epsilon}(S(x',y')))}.$$

[0038] For the optimization process, again any adapted algorithm can be employed.

[0039] The fact that while for registration the optimization objective has to be maximized, the optimization objective has to be minimized for data fusion, reflects the fact that data fusion aims to keep all available information of the input data and to remove the redundant information. In the case of registration, it is just this redundant information, i.e. the information that is present in both input datasets, that is able to drive the registration process towards the optimal spatial correspondence.

[0040] The resulting datasets, $o_{\delta}(T(m_{\alpha}(x,y)))$ and $u_{\epsilon}(S(x',y'))$, are fused thereafter. The final data fusion is a fundamental step with respect to the general design of the system, as it is thanks to the fusion result that the medical doctor or industrial investigator has the impression of being working with only one single physical system. For this aim, the thermal map data, $o_{\delta}(T(m_{\alpha}(x,y)))$, resulting from the previously described signal processing steps, are getting color coded.

[0041] The resulting color mapped thermal data can be overlaid on the structural data, $u_{\epsilon}(S(x',y'))$, resulting in a virtually augmented image. This process is the implementation of the so called "fusion rule" of FIG. 9. It can be programmed by commercially available visualization software packages, like OpenGL or DirectX. These softwares can also be employed for the real-time visualization of the resulting multi-modal data stream.

[0042] Further features and advantages of the invention will appear to those skilled in the art by means of the following description of a particular embodiment in connection with the drawings.

BRIEF DESCRIPTION OF THE DRAWINGS

[0043] FIG. 1 shows a block diagram of the system design.

[0044] FIG. 2 is a block diagram showing in more details the processing system of FIG. 1.

[0045] FIG. 3 shows an illustrative implementation of the system design of FIG. 1. Thermal imaging is performed by a microwave (MW) device; meanwhile an ultrasound (US) device provides the anatomical information.

[0046] FIG. 4 presents the US subsystem of FIG. 3.

[0047] FIG. 5 presents the MW subsystem of FIG. 3.

[0048] FIG. 6 presents in more detail The MW subsystem of FIG. 5. In particular the multi-frequency spiral antennas are shown, which build up the MW transducer.

[0049] FIG. 7 shows how the US and MW transducers are connected.

[0050] FIG. 8 is a block diagram of the image registration process. Either the structural data is getting transformed as outlined in the figure, or alternatively the temperature map is getting spatially transformed on the structural data.

[0051] FIG. 9 is a block diagram of the image fusion process. Thermal map and structural data refer to the already registered data.

[0052] FIG. 1 presents the general design of the system. The data from the different imaging devices are streamed over standard networking or data streaming connection like USB2, IEEE1394, or Ethernet to the processing system. As standard networking connections are being employed, the implemen-

tation of the frame capturing capability of the system is related to the technical specifications of the subsystem or the frame-grabber provider. Necessary device drivers and applications interfaces (APIs) are provided from commercial suppliers.

[0053] If the imaging subsystems have been designed in such a way, configuration information is getting streamed back from the processing system to the imaging subsystems in order to provide the investigator with the impression of being interacting directly with the subsystems. The data from the input devices are getting processed and fused inside the processing system before getting visualized on a computer screen.

[0054] Performing the different image processing steps shown in FIG. 2 continuously as the data arrives over the input networking connections, results in a virtual multi-modal imaging device. The medical doctor or industrial investigator can therefore interpret the acquired multimodal datasets simultaneously and, if the subsystems have been designed in that way, interact with the different subsystems, i.e. the MW and structural devices, as if they were just one single multi-modal device which generates just one single data stream.

[0055] FIG. 2 shows roughly the different image processing steps that are performed by the processing system before on-screen visualization. In more detail, the processing system performs data registration in order to guarantee spatial correspondence of the input data streams, data feature extraction to provide the most pertinent and only pertinent information to the investigator, and data fusion to give the investigator the impression of being working with only one single imaging device. In the following example, these individual digital image processing steps are described in detail for a specific system implementation.

EXAMPLE

Implementation for Liver Tumor Thermal Ablation

[0056] In FIG. 3, a specific system setup for the monitoring of thermal ablation of liver tumors is lined out. Liver is one of the major tumor sites in the western world with an incidence of 680'000 cases/year. During thermal ablation of liver cancers, thin needles are introduced percutaneously until their tips reach inside the tumor volume. At the tips, radiofrequency heats the tumor tissue up to a temperature guaranteeing cell death. In this procedure, two characteristics are fundamental for the success of the treatment: On the one hand, all the cancerous tissue has to be killed, and on the other hand, as few healthy tissue as possible should be ablated. For this, real time monitoring of anatomy, needle positions, and temperature profiles should be provided, which is done with the specific system implementation presented herein.

[0057] There are two imaging subsystems connected to the processing system implemented on a state-of-the-art personal computer (PC): On the one hand, a microwave (MW) imaging device which provides 2D intra-body temperature maps of the patient, and on the other hand an ultrasound (US) imaging system which images 2D slices of the patient's anatomy and the needle positions. As schematically shown in FIGS. 3, 4 and 5, both systems are connected to the PC through real-time networking connections through which the anatomical data and temperature maps are streamed in real-time. For this, the US device uses a USB2 connection, while the MW system employs a Firewire connection.

[0058] The Personal Computer (PC) 4 is provided with following components:

[0059] US device drivers and C++-APIs for USB2 communication from Telemed (see ref. [1]);

[0060] Firewire drivers and C-APIs from Unibrain (see ref. [6]);

[0061] Software for multimodal data registration,

[0062] VTK for data fusion and visualization (see ref. [12]);

[0063] Qt for graphical user Interface (see ref. [13]).

[0064] Using commercially available drivers and C/C++ application interfaces (APIs), the specifications of which may be found in ref. [1] and ref. [6], the processing system receives in real-time the respective datasets from the connected subsystems. The APIs are called from individual C-threads on the PC 4 which are implemented in order to receive the data from the individual imaging subsystems individually, but in a synchronized fashion.

[0065] The employed US subsystem is the commercially available Echoblaster 128 produced by Telemed, Lithonia (see ref. [1]). The two dimensional US frames are streamed over the USB2 connection 3 from the US beamformer 2 to the PC 4, and changes in configuration are streamed back from the PC 4 to the beamformer 2. Furthermore, Telemed provides the hardware drivers and C++ application interface (API) for Windows, based on the DirectX technology from Microsoft. A variety of US transducers 1 is also proposed by Telemed, enabling any programmer to easily implement a fully functional PC based US device.

[0066] FIG. 6 depicts the hardware components of the MW imaging subsystem. The constructed microwave subsystem comprises an array 7 of multi-frequency spiral MW antennas as disclosed by Jacobsen and Stauffer in ref. [2]. The signal sensed by the individual antennas passes through individual Dicke null-balancing radiometers 8, as described by Jacobsen and al. in ref. [3]. The analogue signal from each radiometer 8 is directly related to the brightness temperatures at the locations sensed at different frequencies. An embedded analogue-to-digital converter 9 from Orsys, such as the ORS-116 (see ref. [5]), converts these analogue brightness temperatures into their digital representations. As the analogue-to-digital converter 9 has several analogue inputs, the brightness temperatures from the different antennas can be digitized consecutively. The result is a two dimensional grid of brightness temperatures, where the number of grid points are determined by the number of frequencies that can be sensed by the individual antennas, and the number of antennas that are connected in the antenna array 7.

[0067] The brightness temperatures are directly related to the real intra-body temperatures at the different locations. In order to reconstruct a two dimensional grid of real intra-body temperatures from the brightness temperatures, the algorithm disclosed by Jacobsen and Stauffer in ref. [4] is getting applied to the output grids from the Orsys analogue-to-digital converter 9. In fact, as the algorithm of ref. [4] reconstructs 1D temperature profiles, it is applied consecutively to the brightness temperatures of the individual antennas in the antenna array 7. The combination of the reconstructed 1D temperature profiles results in a 2D temperature map. The reconstruction algorithm from ref. [4] is implemented on the embedded Compact C6713 system 10, sold by Orsys (see ref. [5]). The analogue-to-digital converter 9 from Orsys can actually be plugged directly on the microbus of the Compact C6713 embedded system 10. Consecutive frames of 2D tem-

perature maps are streamed over the firewire connection **5** of the Compact C6713 system to the firewire connector of the PC **4**, while system configuration parameters are streamed back from the PC **4** to the Compact C6713 embedded device. On the PC **4**, the firewire drivers and C-APIs from Unibrain (see ref. [6]) provide the programmer with an easy to use tool to implement a completely functional temperature monitoring imaging device.

[0068] In order to overlay the temperature maps from the MW device on the US frames with a guaranteed spatial correspondence, the US transducer **1** is physically linked to the MW antenna array **7**. This guarantees that both datasets are acquired within the same imaging plane and that the imaged regions of both devices overlap significantly. The link between the two transducers is outlined in FIG. **7**. The two transducers are connected through a rotational joint **11**, which allows adapting the rotational angle α according to the local patient's anatomy, e.g. curved or straight skin surface **12**. As a result, the two datasets lay both in the same imaging plane, but are mutually rotated by an angle α . The field of view of the MW antenna array **7** is indicated by **15** and the field of view of the US transducer **1** is indicated by **16**. The analogue connection between US transducer **1** and beamformer **2** is indicated by **14** and analogue connection between antenna array **7** and system **6** is indicated by **13**. Therefore, before a data overlay with spatial correspondence can be provided, this angle α has to be determined in order to compensate for the rotational difference. This process of bringing the two datasets into spatial correspondence provides data registration. The specific implementation of the registration algorithm is implemented on the PC **4**.

[0069] The registration process which enables to compensate for the rotational offset of a between the US and MW scans is outlined in FIG. **8**. The system streams via connections **5** and **3** on the one hand the thermal data from the MW device **6**, noted $T(x,y)$, and on the other hand the structural data from the US device **2**, noted $S(x',y')$ to the signal processing PC **4**. x and y , resp. x' and y' , parameterize the discrete imaging space of the thermal MW data T , resp. the structural US data S , as described in the previous paragraphs. As depicted in FIG. **7**, the imaging space of the MW data and the imaging space of the US frames differ by a rotational angle α . In order to find continuously a spatial correspondence between both, the varying angle α shall be continuously determined in order to compensate for it. This corresponds to determining the mapping $m_\alpha: (x',y') \rightarrow (x,y)$, with a being the single valued rotational transformation of the mapping. The datasets S and T represent different information about the investigated patient, and the determination of this mapping is described in the following and conceptually outlined in FIG. **8**.

[0070] In fact both, the rotational angle α and image features which allow the determination of α have to be determined simultaneously. This is because by nature of the two imaging modalities, the raw data does not contain corresponding information which allows direct mutual registration. Rather, the data features which represent pertinent information for the determination of the rotational angle α have to be determined. As disclosed in this invention, the determination of the registration parameter α and of the features pertinent to the determination of α are done simultaneously.

[0071] The feature extraction step can have a variety of specific implementations, e.g. considering prior information about the features to be extracted, discretely or continuously

parameterized features, etc. With respect to the specific implementation described in this example, the feature extraction parameters β and γ represent a particular scale of the scale space image decomposition described by Lindenberg in ref. [7]. The feature extraction block within the multimodal registration process detects the image features most pertinent for the determination of the spatial correspondence between the input images and removes those not being of any use. The fact that in this particular implementation the imaging features are restricted to a specific scale of the scale space decomposition of the initial datasets reflects a known prior information about which image features will result in good registration. Still, the exact scale is not being fixed from the beginning, as the best scale in the scale space decomposition is not guaranteed to remain constant. Rather, it might change with changing parameters in the image acquisition process, such as e.g. a changing frequency used for the US image acquisition, since Teleded provides multi-frequency US transducers.

[0072] The optimization objective which allows simultaneous extraction of the best scale of the scale space image decomposition, i.e. the best features for the spatial registration, and the determination of the optimal registration angle α is called feature efficiency and is written

$$e(F_T, F_S) = (I(F_T, F_S) / H(F_S, F_T))$$

as indicated above. F_T is estimated from the thermal data T , and F_S is estimated from the structural data S , according to the teaching of Thomas A. Cover in ref. [8]. Histogramming is being employed as the probability estimator for F_T , F_S , and the joint random variable $F_{T,S}$ as described by T. Butz in ref. [9]. This means that the following formulas are being employed to estimate the probability densities, p_S , p_T , and $p_{S,T}$, for the random variables F_S , F_T , and $F_{S,T}$ respectively:

$$p_S(f_S) = \frac{1}{N} \sum_{x,y} \delta_{f_S(x,y), f_S},$$

$$p_T(f_T) = \frac{1}{N} \sum_{x,y} \delta_{f_T(x,y), f_T},$$

$$p_{S,T}(f_S, f_T) = \frac{1}{N} \sum_{x,y} \delta_{f_S(x,y), f_S} \delta_{f_T(x,y), f_T},$$

where N is the number of features in the datasets. $\delta_{a,b}$ is the Kroenecker delta function, which is 1 if $a=b$ and 0 otherwise. Other probability estimators might be used as well, such as Parzen-window probability estimation. The probability estimation step is important to the registration process of FIG. **8**, as the information theoretic measures can be evaluated and optimized using these probability densities.

[0073] The action of adapting registration parameters and image features refers to adapting the parameters α , β , and γ . For maximization, an optimization algorithm such as Powell (see ref. [10]) or genetic optimization (see ref. [11]) can be used.

[0074] In contrast to the data feature extraction related to image registration as described in the previous paragraph, the feature extraction for data fusion aims to extract the features of the initial datasets which are most complementary to each other while removing redundant information from the datasets. The feature extraction from the input thermal maps, resp. the US data, is represented by a mapping $o_S: T(m_\alpha(x, y)) \rightarrow o_S(T(m_\alpha(x, y)))$, resp. $u_\epsilon: S(x', y') \rightarrow u_\epsilon(S(x', y'))$. δ , resp.

ϵ , represent again a particular scale of the scale space decomposition according to ref. [7] of the initial MW thermal maps, $T(x,y)$, resp. the anatomical data of the US device, $S(x',y')$. The extraction process is driven by the minimization of the same optimization functional e as in the previous paragraph.

[0075] For the optimization process again, an algorithm, such as Powell or genetic optimization, can be employed. The resulting datasets, $o_\delta(T(m_\alpha(x,y)))$ and $u_\epsilon(S(x',y'))$, will be fused thereafter.

[0076] For the data fusion, the thermal maps, $o_{67}(T(m_\alpha(x,y)))$, resulting from the previously described signal processing steps, are color coded so as to reflect a natural interpretation, e.g. hot spots being red and cold spots being blue. When a thermal data, $t(x,y)=o_{67}(T(m_\alpha(x,y)))$, is initially represented by a scalar within $[t_{min}, t_{max}]$, such a thermal mapping is being performed by the following color coding equation:

$$\begin{pmatrix} r \\ g \\ b \end{pmatrix}(x, y) = \begin{pmatrix} 0 \\ 2 \cdot t(x, y) / t_{max} \\ 1 - 2 \cdot t(x, y) / t_{max} \end{pmatrix}, t \in [t_{min}, t_{max} / 2],$$

$$\begin{pmatrix} r \\ g \\ b \end{pmatrix}(x, y) = \begin{pmatrix} 2 \cdot t(x, y) / t_{max} \\ 1 - 2 \cdot t(x, y) / t_{max} \\ 0 \end{pmatrix}, t \in [t_{max} / 2, t_{max}].$$

[0077] The resulting color mapped thermal data can be semi-transparently overlaid on the structural data, $u_\epsilon(S(x',y'))$, resulting in a virtually augmented image. In this example, the software VTK (Visualization Tool Kit) (see ref. [12]) is employed as the data fusion and visualization package.

[0078] The software Qt available from Trolltech (see ref. [13]) is being employed for the implementation of the graphical user interface, which is designed in a way that the doctor can interact directly over the USB2, resp. Firewire, connection to the US device, resp. MW device, with the imaging subsystems. Thus, performing the described different image processing steps continuously as the data arrive over the input networking connections, results in a virtual multi-modal imaging device. The doctor can therefore interpret the acquired multimodal datasets simultaneously and interact with the MW and US subsystems, as if they were just one single multi-modal device which generates just one single data stream.

[0079] The invention as described herein above is capable to provide the industrial investigators and medical doctors simultaneously and in real-time, or off-line, with both structural data on the one hand and thermal maps on the other hand. Furthermore, as the information from different imaging modalities is combined by the multimodal signal processor, also the pertinent and complementary information from the different modalities is combined, resulting in a virtually augmented single system with increased value versus the individual subsystems.

[0080] The open standard technology of the data stream connections between the individual data acquisition systems and the processor enables removal and addition of imaging subsystems according to need and comfort of the industrial

investigators or medical doctors. This applies to 1D, 2D, 3D or mixed data and data sequences.

REFERENCES

- [0081]** [1] <http://www.telemet.it>
- [0082]** [2] S. Jacobsen and P. R. Stauffer
- [0083]** Multifrequency Radiometric Determination of Temperature Profiles in a Lossy Homogeneous Phantom Using a Dual-Mode Antenna with Integral Water Bolus
- [0084]** IEEE Transactions on Microwave Theory and Techniques, vol. 50, no. 7, pp. 1737-1746, July 2002.
- [0085]** [3] S. Jacobsen, P. R. Stauffer, and D. Neuman
- [0086]** Dual-mode Antenna Design for Microwave Heating and Noninvasive Thermometry of Superficial Tissue Disease
- [0087]** IEEE Transactions on Biomedical Engineering, vol. 47, pp. 1500-1509, November 2000.
- [0088]** [4] S. Jacobsen and P. R. Stauffer
- [0089]** Nonparametric 1-D Temperature Restoration in Lossy Media Using Tikhonov Regularization on Sparse Radiometry Data
- [0090]** IEEE Transactions on Biomedical Engineering, vol. 50, no. 2, pp. 178-188, February 2003.
- [0091]** [5] <http://www.orsys.de>
- [0092]** [6] <http://www.unibrain.com>
- [0093]** [7] T. Lindeberg
- [0094]** Scale-space theory: A basic tool for analyzing structures at different scales
- [0095]** J. of Applied Statistics, vol. 21(2), pp. 224-270, 1994
- [0096]** [8] Thomas A. Cover
- [0097]** Elements of Information Theory
- [0098]** Wiley-Interscience
- [0099]** [9] T. Butz
- [0100]** From Error Probability to Information Theoretic Signal and Image Processing
- [0101]** Thèse No. 2798, ITS, EPFL
- [0102]** [10] William H. Press
- [0103]** Numerical Recipes in C
- [0104]** Cambridge University Press
- [0105]** [11] <http://lancet.mit.edu/ga/>
- [0106]** [12] <http://www.vtk.org>
- [0107]** [13] <http://www.trolltech.com>

1. A virtual multimodal non-invasive imaging device comprising:

- a first monomodal, non-invasive microwave imaging subsystem with first sensing means and with first processing means, providing digitized microwave intra-body thermal map data from a sensed body,
- a second monomodal, non-invasive imaging subsystem with second sensing means and with second processing means, providing digitized intra-body structural map data from said sensed body, and
- a multimodal signal processor performing spatial registration of thermal and structural maps, data fusion into a multimodal data set and visualisation of said multimodal data set,

wherein said multimodal signal processor includes a feature extraction which detects and selects the image features most pertinent for the spatial correspondence of the input images, and

wherein said processor uses information theoretic measures between said image features in order to perform spatial registration of said thermal map with said structural map.

2. A device as claimed in claim 1, wherein the data sets of the first and second monomodal subsystems lay both in the same imaging plane.

3. A device as claimed in claim 1, wherein the data sets of the first and second monomodal subsystems are getting processed and fused inside the processing system before getting visualized on a computer screen.

4. A device as claimed in claim 1, wherein said information theoretic measures between said image features are mutual information, normalized entropy or feature efficiency.

5. A device as claimed in claim 1, wherein said processor extracts corresponding or complementary image features of said thermal map and of said structural map for the registration process or for the data fusion step, respectively.

6. A device as claimed in claim 1, wherein the thermal data of said multimodal data set are color coded and overlaid to the structural data.

7. A device as claimed in claim 1, wherein configuration information is streamed back from said processing system to said imaging subsystem.

8. A device as claimed in claim 1, wherein said microwave imaging device comprises an array of multi-frequency microwave antennas associated to Dicke null-balancing radiometers and an analogue-to-digital converter.

9. A device as claimed in claim 8, wherein said microwave imaging device is connected to said processor by a firewire connection.

10. A device as claimed in claim 1, wherein said second imaging subsystem is a non-invasive ultrasound subsystem.

11. A device as claimed in claim 10, wherein said ultrasound subsystem is connected to said processor by a USB2 connection.

12. A device as claimed in claim 1, wherein in order to bring the data into spatial correspondence, a sensor of said microwave imaging device or said first sensing means and a sensor of said structural imaging device are connected mechanically.

13. A device as claimed in claim 12, wherein said sensors are connected by means of a rotational joint.

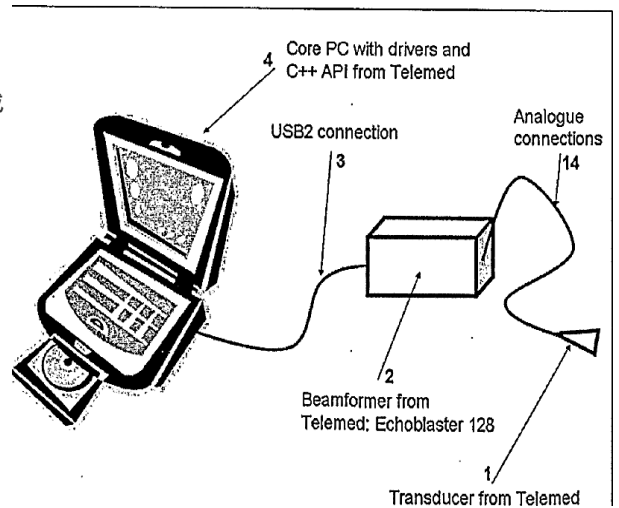
14. A device as claimed in claim 1, wherein in order to bring the data into spatial correspondence, a software tool performs this task by maximizing an information theoretic measure between image features with respect to possible image rotations and displacements.

* * * * *

专利名称(译)	结构数据的温度映射		
公开(公告)号	US20080139931A1	公开(公告)日	2008-06-12
申请号	US11/795457	申请日	2006-01-13
[标]申请(专利权)人(译)	IMASYS		
申请(专利权)人(译)	IMASYS SA		
当前申请(专利权)人(译)	PIXARTIS SA		
[标]发明人	BUTZ TORSTEN THIRAN JEAN PHILIPPE KUNT MURAT		
发明人	BUTZ, TORSTEN THIRAN, JEAN-PHILIPPE KUNT, MURAT		
IPC分类号	A61B5/00 A61B8/00		
CPC分类号	A61B5/015 A61B5/0507 A61B8/08 G06T2207/30004 G06T7/0028 G06T7/0034 A61B8/5238		
优先权	2005405026 2005-01-17 EP		
外部链接	Espacenet USPTO		

摘要(译)

已经认识到温度成像改善了各种诊断和介入程序并且预测和防止电路和设备的故障。公开了一种系统设计和方法，其中热数据与来自US，CT或MR扫描仪的数据流融合和映射，给医生或工业研究者提供与已知的美



国，CT或MR系统已通过温度映射功能得到增强。